USING MULTI-SCALE MONITORING TECHNOLOGY TO EVALUATE REMEDIATOIN EFFICIENCY IN SHIH-MEN RESERVOIR WATERSHED

Bor-Shiun Lin, Cheng-Yang Hsiao, Chun-Kai Chen, Chen-Kun Hsu, Chin-Tung Cheng

Disaster Prevention Technology Research Center, Sinotech Engineering Consultants, Inc., Taiwan

ABSTRACT

This study utilized the multi-scale monitoring technology which incorporated field investigations to establish reliable real-time data for validating the efficiency of Shih-men watershed's management project. The management project aims to reveal vegetation recovery, extent of soil and water conservation, and the reduction of sediment yields as well as to mitigate the sediment disasters and trace topological changes. The results show that all of the engineered watersheds have met the above expected targets and that sediment discharges are under control.

Index Terms— *Shih-men watershed, sediment disaster, multi-scale Monitoring, management efficiency*

1. INTRODUCTION

The recent global climate change dramatically increased natural disasters. Of those, many were compound disasters. In northern Taiwan, Shih-men Reservoir is a critical infrastructure that provides potable water to resident. Shih-Men Reservoir began operation in June, 1964. During the flood seasons of 2001 to 2005, typhoons Toraji, Nari, Aere, Haitang, Matsa, Talim, and Longwang struck Taiwan and caused serious sediment disasters. Masses of sediment were washed into the reservoir, resulting in increased turbidity both in the reservoir and rivers within the watershed. This far exceeded the capacity of the Shih-Men water treatment plant, triggering a severe water shortage. It had tremendous impacts on the Taiwan public and industry. To solve this problem, Legislative Yuan passed "Special Statute for managing and remediating Shih-Men Reservoir watershed and its catchment area.

In accordance with the "2006 to 2011 Shih-Men Reservoir Watershed and its Catchment Remediation Plan" relevant agencies were asked to propose multipurpose remediation plans. The primary goals of the proposed plans are to reduce reservoir turbidity levels, extend the life of the dam and improve remediation efficiency. Watershed conservation and remediation can be separated into two periods: The first period was implemented from 2006 to 2009 and primarily focused on the remediation of exposed landslide scarps and placement of check dams. The second period was implemented from 2009 to the current year, 2011, and was primarily focused on the vegetative recovery of slopes. The study aims to uses a multi-scale monitoring technique paired with field measurements to produce time referenced sediment migration data .and then uses this data to validating the efficiency of Shih-men watershed's management project..

2. STUDY AREA

Shih-men Reservoir watershed has an unique terrain and geology. Furthermore, it has a complex river system and fairly steep slopes. These are compounded by heavy rainfalls and typhoons in Taiwan so that landslides occur frequently. This study chooses Sule catchment from Shih-men Reservoir watershed and it locate at central part of the watershed as shown in fig.1. The topological characteristics and hydrological condition, and historical landslides are described as below.

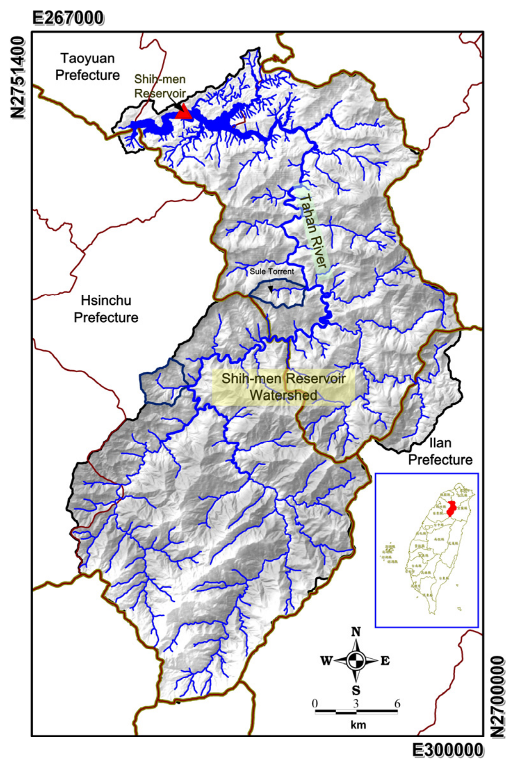

Fig.1 Geographical Locations of Shih-men Reservoir Watershed.

Shih-men Reservoir watershed terrain is narrow and long, going from south to north. Most of its formation is sedimentary rocks and mild metamorphic rocks. Its fold lines and faults go from northeast to southeast. Almost all of its soil is stony soil, and the slope angle is mostly at 20 to 45 degree. Most of them are coniferous and broadleaf forests. It consists of mostly national forest compartments.

The mainstream in the Shih-men Reservoir watershed is the Tahan River basin, upstream from the Tamsui River. It originates in the Hsuehshan Range and goes through Amuping into the Western Foothill. It has many tributaries with irregular patterns. The watershed is exposed to the subtropical monsoons with higher humidity and greater temperature changes. Over 25 years worth of rainfall data within the Shih-men Reservoir watershed were collected. Hydrological analysis was conducted. The result suggests the heaviest single-day rainfall fell within the southwestern part of the watershed (see fig.2). The historical trend of annual average rainfalls in Shih-men Reservoir is shown in fig.3. It can be found the average rainfall has markedly increased for the past ten years. This is especially after 2004 Typhoon Aere, where the annual average rainfall is the greatest in Taiwan. The recent climate change is very obvious.

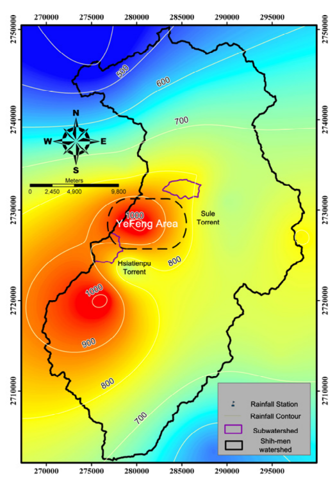

Fig.2 Distribution of rainfalls intensity in the 50 year return period

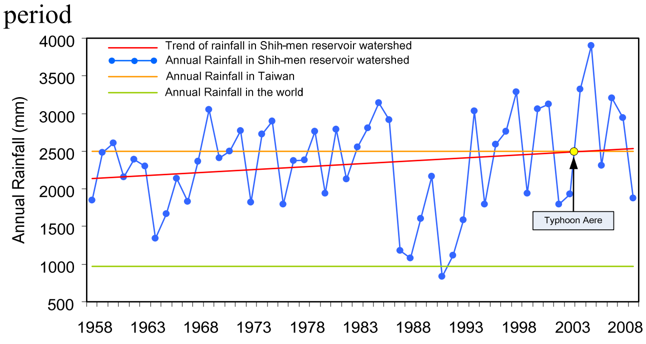

Fig.3 Average annual rainfalls in Shih-men Reservoir watershed

SWCB (2010) indicated that first stage remediation projects center around the reservoir itself and Yufeng watershed. The first stage remediation and conservation projects become more active after Typhoon Aere. Among them, Sule catchment is a typical remediation area. Sule River is situated in Fuxing Township of Taoyuan County. It intersects the Sule Bridge on Provincial Road Tai 7 Line. The watershed area is approximately 5.96 km^2. The recent typhoons and heavy rains have caused a series of disasters, triggering serious sedimentation and erosion in the watercourse. Debris destroyed Sule Bridge, its surrounding farms, and nearby roads several times. Since 1996, the Sule watershed has been frequented by many typhoon rains. However, of those typhoons, three caused major landslide and debris flows to occur: Typhoon Aere (2004/08/23), Typhoon Haitang (2005/07/16) and Typhoon Matsa (2005/08/03). Rains associated with these storms exceeded the 24 hour rainfall of a 10 year storm in Taiwan. Rainfall patterns associated with typhoon Matsa were especially intense and caused rapid stream height increases and landsliding in the source area of the Sule catchment. These intense rainfalls also reduced shear strengths of soils and caused shallow slope failure in the weathered rock of the source areas and serious sediment disasters Rainfall associated with Typhoon Aere were also incredibly intense. 24 hour accumulated rainfall exceeded 1000 mm and caused the most serious damage to the Sule watershed. Stream banks simultaneously failed and the downstream Sule bridge was swept away be resulting debris flow. In total, 21.6 ha of landslide area were created during Typhoon Aere shown in fig. 4.

Through landslide interpretation of satellite images, the sliding area prior to the Chi-Chi earthquake is about 1.29 ha. From post Chi-Chi earthquake satellite images after various typhoon events, including typhoon XANGSANE, typhoon TORAJI, typhoon NARI and Typhoon AERE, the changes in sliding area were analyzed. Fig. 5 shows the change in landslide area in these typhoon events. It is deserved to be mentioned that landslide area caused by typhoon AERE is about 21.84 ha, compared to 16.48 ha due to typhoon TORAJI. The spatial distribution of landslide is presented in fig. 4. It may be noted that most of the slides occurred along the river channel due to erosion of river banks when the water level is high (see fig. 6). After Typhoon Aere, SWCB start to plan remediation engineering for the environmental restoration. Since 2006, and the initiation of the Shimen reservoir remediation plan, six separate engineering works have been completed in the Sule catchment as shown in fig. 4. The aim of the projects has been divided into two categories: Debris flow restoration works and debris flow re-construction works. Those works included check dam, river bed foundation, and riverbank retaining wall construction as well excavation of deposited sediments. At the same time, monitoring was performed for evaluating the remediation efficiency. The following section will introduce how to use multi-scale monitoring to validate the above.

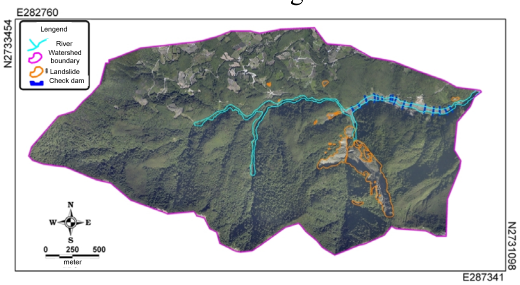

Fig. 4. Spatial disribution of landslide induced by Typhoon Aere in Sule catchment

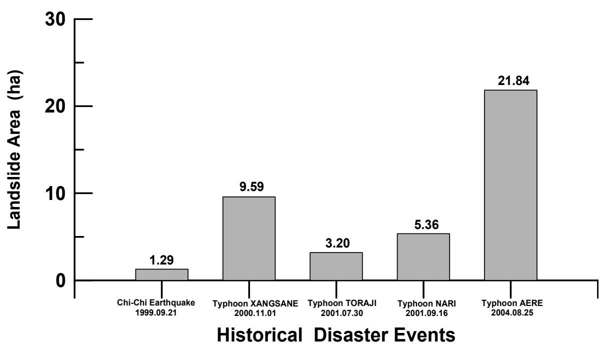

Fig. 5. Bar chart of landslide area change in historical disaster events in Sule catchment

(a) Aerial photo of Suler catechment in upstream

(b) Shallow landslide near Route No. 7

Fig. 6. Photos of landslide in Sule catchment after Typhoon Aere

3. MULTI-SCALE MONITORING

Presently, the greatest challenge of Shih-Men Reservoir is sedimentation. Whether caused by human development or natural factors, it directly triggers problems such as increased turbidity and reduced reservoir storage volume. It also affects the transportation systems,, watercourse, and water supply. Sediment source can be classified into four categories (see fig. 7) and is described below:

(1) Soil erosion ： Caused by surface runoff and pronounced on bare slopes of soil consisting of fine particles.

(2) Landslides and debris flows ： Sediment materials from landslide and debris flows in the watershed may be the primary source. Increases in flow cause increased amounts of fine suspended particles to enter the mainstream as well as the reservoir itself.

(3) Long-term deposition in riverbed ： During storms, settled fine particles become agitated. This is particularly apparent in the upstream check dam area of Shih-Men reservoir, which in the past has accumulated large deposits of fine material and is a major source of turbidity.

(4) Unstable slope along road ： Fine contents from unstable slope deposits becomes agitated, erode during peak storm flows and are carried by water into the reservoir.

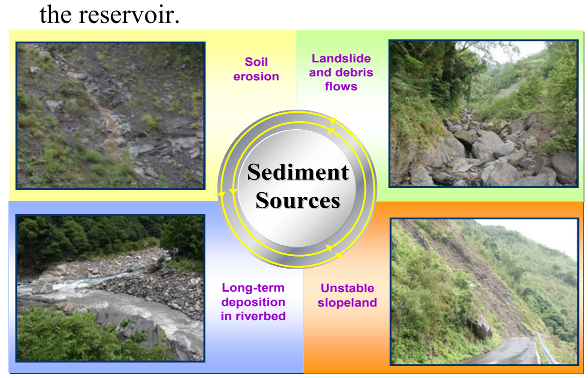

Fig. 7 Diagram of sediment sources in Shih-men reservoir watershed

Multi-scale monitoring was to use in Shih-men reservoir watershed to study remediation efficiency and the topographical changes before and after remediation and flood seasons. This allows for comprehensive understanding of sediment changes and sediment yield estimation to quantify the remediation efficiency. This study estimated both local and overall sediment productions, including using erosion pin to monitor soil loss on different surfaces. Telemetry was complemented by airborne LiDAR to calculate failure volume and sand trapping capacity. High-resolution images from multiple periods were used to study the extent of surface vegetation to demonstrate the effectiveness of watershed remediation and restoration. In this study, sediment materials main supplies by soil erosion and landslide. Afterward, the monitoring focus on fine soil content retention and vegetation of them and those procedure and methods are described in below.

3.1. Sediment sources form soil erosion

Soil erosion estimates, on the other hand, were often based on empirical equations, such as Universal Soil Loss Equation (USLE), Modified Universal Soil Loss Equation (MUSLE), etc. (Wischmeier and Smith, 1960; Williams, 1975). These empirical equations are limited regionally and by spatial distribution of rainfalls. Moreover, they only represent the averaged results of overall watershed erosion and can not be used to study the individual regional management. Therefore, this study focused on the different vegetated slopes to design erosion pins by some research reports (Schumn, 1956; Crouch, 1987; Lawler *et al*., 1997). Site surveys were conducted to measure surface erosion depth to investigate the state of slope soil after erosion from rainfalls. The result was used to assess the inhibition rate of soil erosion from both remediated and non-remediated hillslopes in order to understand the efficiency of remediation. To quantify the soil erosion retention ratio (*SLR*) from the measured soil erosion depth of several erosion pins (see fig. 8) embedded in remediated and non-remediated hillslopes, one used an index value to depict efficiency of soil erosion retention after completing remediation. Higher index values indicate higher soil erosion retention. Therefore, this study uses this index (*SLR*) to understand the remediation efficiency of the hillslopes. *SLR* would is defined as follows

$$SLR(\%) = \frac{E_{DR} - E_{DN}}{E_{DR}} \times 100\% \qquad (1)$$

Where SLR is soil erosion retention ratio (%)；E_{DR} is surface eroded soil depth of remediated hillslope (mm)；E_{DN} is surface eroded soil depth of non-remediated hillslope (mm).

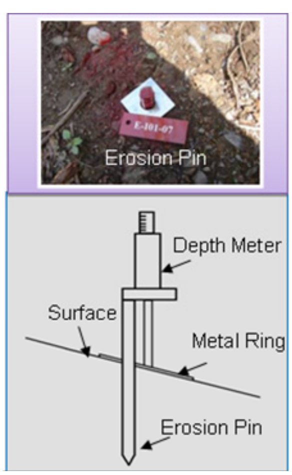

Fig. 7 Schematic layout of erosion pins

3.2. Sediment sources form landslide

To understand the evolution of failures in space and in time of the Shih-men watershed, this study compiled satellite images to identify the landslide distribution. Number of landslides, existing landslide area, incremental landslide area, and spatial distribution in key regions were obtained through digital interpretation to understand its evolution. Further, this was complemented with multi-period terrain data, established by airborne LiDAR, to quickly obtain information on terrain changes in each sub-catchment area and assess the effectiveness of the remediation projects. This study adopted multi-band high-resolution images from different periods to analyze the ratio of green cover to assess the vegetation restoration after remediation. Normalized Difference Vegetation Index (NDVI) is currently a popular method to assess vegetation coverage (Kriegler *et al*., 1969; Green *et al*., 1997). The NDVI is calculated from these individual measurements as follows:

$$NDVI = \frac{NIR - VIS}{NIR + VIS} \times 100\% \qquad (2)$$

where VIS and NIR stand for the spectral reflectance measurements acquired in the visible (red) and near-infrared regions, respectively.

Moreover, the required technology is nearly perfected and can be broadly applied to vegetation coverage classification and study. Therefore, this study used NDVI of satellite images from the periods before Typhoon Morakot, after Morakot, and after Typhoon Parma to assess the vegetation restoration in Shih-men watershed. The study used ArcGIS to complement the interpretation of non-vegetation areas (buildings, lakes, roads, bare lands, rice fields, and point cloud etc.) or areas that need to be excluded, to establish a reasonable threshold for the vegetation samples. Once the threshold was defined from these satellite images', the NDVI could be used to classify the images into vegetated and non-vegetated. The ratio of green cover is the percentage of vegetation coverage of the total area, as shown in Eq. (3).

$$GR(\%) = \frac{A_V}{A_C} \times 100\% \qquad (3)$$

Where GR is the ratio of green cover; A_c is a given catchment area, and A_v is vegetated area within a given catchment.

To evaluate the efficiency of check dams, this study utilized LiDAR (Laser Detection and Ranging) technology to survey and produce high resolution DEMs of the Shih-men reservoir watershed. The DEM construction procedure is shown in fig. 8. The pre-event DTM is subtracted from the post-event DTM. A negative value in the grid represents failure or erosion, and positive value indicates deposits. Variation in volume of a grid can be obtained by multiplying this value by the area of the unit grid (see fig. 9). The total volume of landside material and sediment trapped by the check dam can also be obtained from multiple LiDAR generated DTMs. Then, sediment discharge and trapping efficiency of dams can be precisely calculated. It can also be applied to monitor the accumulated volume of sediment on the confluence between tributaries and river, growth of alluvial fan, and large scale wedge like slope failures. Comparison of LiDAR DEMs from different periods can also indicate terrain migration and be used to trace sediment transport from tributaries, especially in extreme typhoon disaster. Sediment trapping ratio (STR) can be assessed by measuring the volume of deposited sediment in front of the check dams (Sophie *et al.*, 2008; Lin, 2010). If *STR* is close to or over 60%, it means that check dams are effectively controlling sediment transport and have adequate remediation efficiency levels. The sediment trapping ratio can be expressed as：

$$STR(\%) = \frac{V_d}{V_y} \times 100\% \qquad (4)$$

Where V_d is the trapped volume in the check dam(m^3)；V_y is the sediment yield from upstream (m^3).

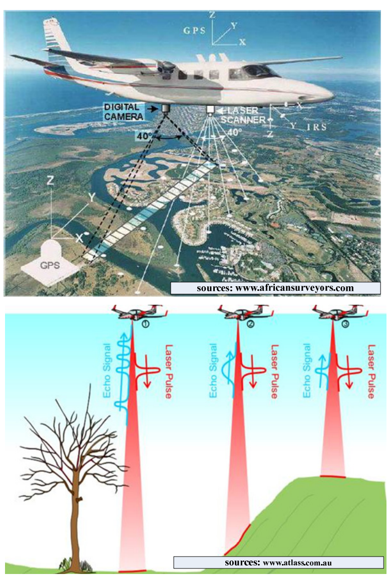

Fig. 8 Schematic layout of air-borne LiDAR technology

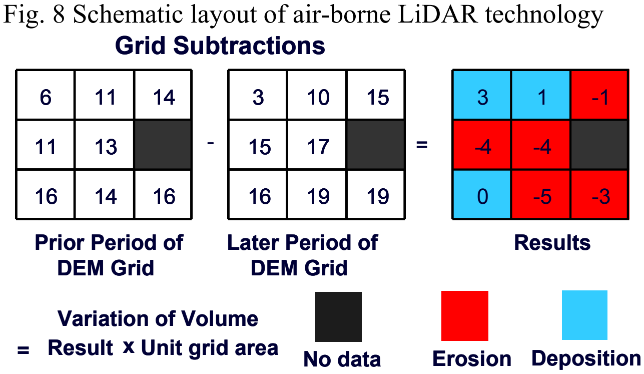

Fig. 9 Grid Subtractions between DEM from prior period and later period (from Hsiao *et al.*, 2011)

4. RESULTS OF MANAGEMENT EFFICIENCY

This section uses the multi-scale monitoring technology which incorporated field investigations to establish spatio-temporal field data to quantify soil erosion and sediment yield for validating the efficiency of remediation of Sule catchment.

4.1 Soil erosion retention

To effectively measure surface soil loss on remediated and non-remediated hillslopes chosen one site to put ten erosion pins to monitor eroded soil depth for each rainfall events. The locations and photos of two sites are displayed in fig. 10 and fig. 11. The monitoring period is from Sep., 2008 to Dec., 2010. Fig. 12 is the diagram of the average annual accumulated eroded soil depth on remediated and non-remediated hillslopes. According to the figure, soil erosion of remediated hillslopes is obviously lower than the remediated. Compared with others, remediated hillslopes can reduce soil erosion about 1.6 mm. Those data are input into Eq. (1) and then *SLR* of Sule catchment could be obtained as below：

$$SLR(\%) = \frac{7.1 - 5.5}{7.1} \times 100\% = 22.53\% \qquad (5)$$

The above result shows that remediation of hillslops could reduce annual amounts by 22.53% of soil loss per unit area. It is evident that remediation would accelerate environmental vegetation recovery and under good control.

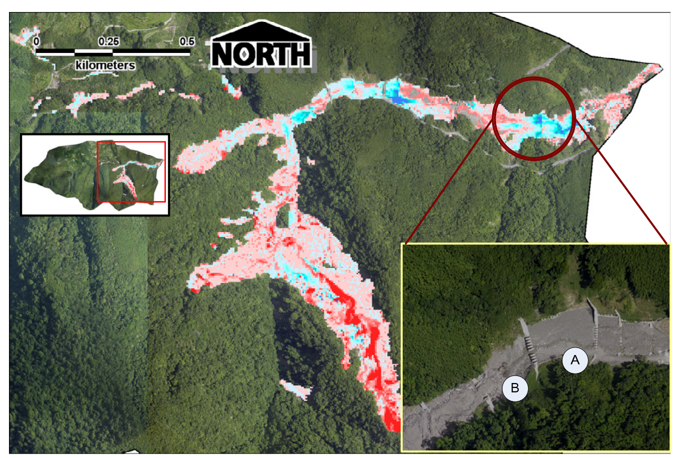

Fig. 10 Locations of two sites for monitoring soil erosion

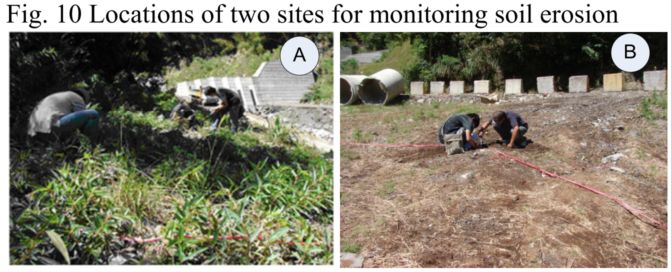

Fig. 11 Photos of monitoring soil erosion on remediated and

non-remediated hillslopes in Sule catchment.

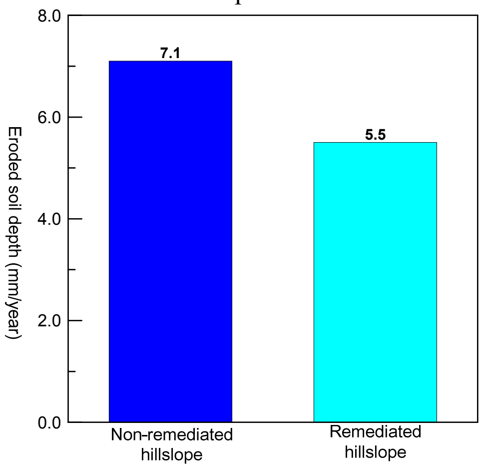

Fig. 12 Diagram of average annual eroded soil depth on remediated and non-remediated hillslopes.

4.2 Vegetation recovery and sediment trapping ratio

This study used NDVI to assess vegetation recovery of overall Sule catchment after remediation in three periods. The first period is after Typhoon Aere and before Typhoon Morakot, the second is after Typhoon Morakot and before Typhoon Parma and the last is after Typhoon Parma (see fig. 13). According to Eq. 2~3, the ratio of green cover are calculated and shown in fig.14. Although in these periods, Typhoon Morakot and Typhoon Parma affected Sule catchment, the ratio of green cover still maintained over 80% by satellite images. Again, it shows remediation including check dams, river bed foundation, and revetment as well excavation of deposited sediments, has good efficiency.

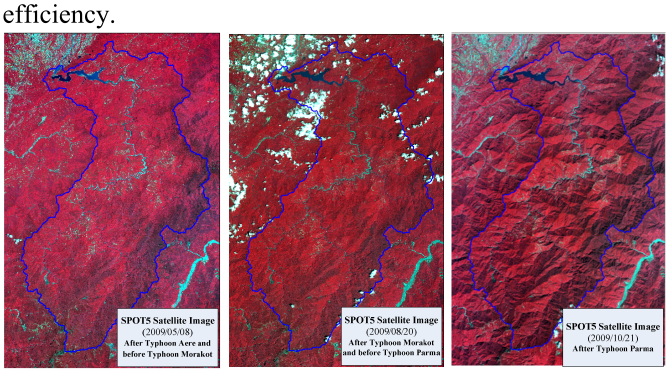

Fig.13 SPT5 Satellite Images from Three Periods.

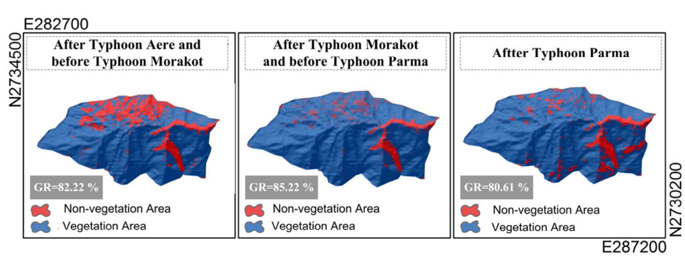

Fig. 14 Variation of ratio of green cover in Sule catchment

Soil and Water Conservation Bureau (2009, 2010, 2011) has conducted four comprehensive airborne LiDAR scans to create high-precision digital elevation models. These measurements can be divided into there measurement periods. Variation of elevation in a grid can be obtained by multiplying this value by the area of the unit grid (see fig. 9). Further, sediment yield is the total volume of terrain changes such as slope failures and river erosions. Sediment trapping ratio (STR) can be assessed by measuring the amount of sediment trapped in front of the check dams. Four DEMs are used to perform comparative analysis for sediment yielded and sediment trapped from different periods to quantify the efficiency of check dames. STR from three periods was obtained and listed in table 1. Further, spatial distribution of landslide area, sediment yields and sediment trapping from different periods of DEMs are shown in fig. 15.

Table1 List of sediment yielded and sediment trapped from different periods in Sule catchment

Period	Incremental landslide area (m^2)	Sediment yield (m^3)	Sediment trapped (m^3)	STR (%)
2006/06 ~ 2008/08	177,836.50	122,646.00	77,271.00	63.00
2008/08 ~ 2008/11	162,089.20	8,426.50	6,285.00	74.59
2008/11 ~ 2009/10	157,692.07	8,968.50	5,946.63	66.31
			Average =	67.96

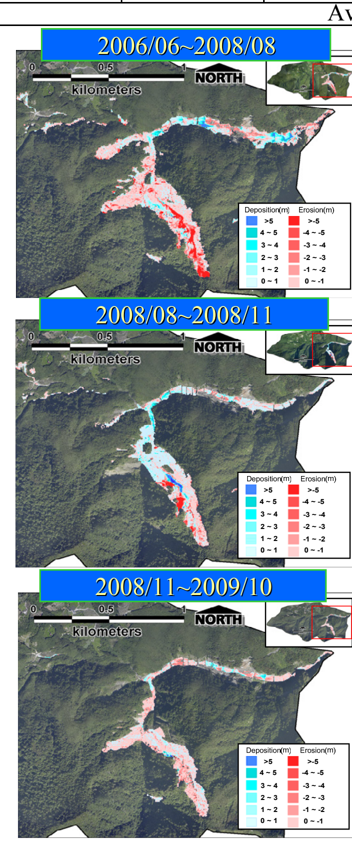

Fig. 15 Spatial distribution of elevation changes in Sule catchment at there periods

Based on the results, incremental landslide area and sediment yield had been reduced by years after remediation of slope and river channel. In general, greater the sediment yield, greater was the amount of sediment trapped. And, STR of Sule catchment from the first period to the third is increasing with time. Although they were slightly lower, they maintained 67.59%. The average STR is greater than 54%, which approaches the expected value of 54% from Shih-men watershed's management project. At the same time, aerial photos also show good vegetation and sediment material under stable situation, as shown in fig. 16. Through the above, it was found that sediment washing into river at upstream was effectively controlled and gradient gentler.

Fig. 16 Spatial distribution of elevation changes in Sule catchment at there periods

5. CONCLUDSIONS

To study the efficiency of remediation projects, field measurement, remote sensing of satellite images and airborne LiDAR technology were all adopted to monitor and analyze environmental vegetation and amount of sediment yield after remediation. The results, which prove the remediation of Shih-men watershed, span a different measurement scales. The main conclusions are summarized as below:

1. Soil erosion and sediment yield estimates quantified based on spatio-temporal field data effectively represent and validate the efficiency of remediation of the Sule catchment.
2. In the study case of Sule catchment, remediation on hillslops reduced annual amounts of soil loss per unit area by 22.53%. In addition, the ratio of green cover still maintained over 80% as determined by satellite images. Also, the average STR value remained in the normal range which approaches the expected value of management project. It is evident that remediation would accelerate environmental vegetation recovery and sediment yields have good control.
3. After the remediation project of Shih-men reservoir watershed, most of the failure restorations were sound. It is hoped that results from the assessment of remediation can be applied to future remediation efforts of other reservoir watersheds.

REFERENCES

[1] Soil Water Conservation Bureau (SWCB), "Study on Historical Migration and Its Mechanism of Heavy Rainfall-induced Sediment Disaster in Shih-Men watershed", 2010 (in Chinese).

[2] Wischmeier, W. H., and Smith D. D., "A Universal Soil-loss Equation to Guide Conservation Farm Planning," *7th International Congress of Soil Science*, Madison, pp. 418-425. 1960.

[3] Williams, J. R., "Sediment Yield Prediction with Universal Equation Using Runoff Energy Factor," *Proceedings of the sediment-Yield Workshop*, USDA Sedimentation Laboratory, Oxford, Mississippi, 1975.

[4] Schumm, S., "Evolution of Drainage Systems and Slopes in Badland at Perth Amboy", New Jersey, *Bulletin of Geological Society of America*, 67, pp. 597-646, 1956.

[5] Crouch, R. J., "The Relationship of Gully Sidewall Shape to Sediment Production," *Australian Journal of soil Research*, 25, pp. 531-539, 1987.

[6] Lawler, D.M., Couperthwaite, J., Bull, L.J., and Harris N.M., "Bank Erosion Events and Processes in the Upper Severn Basin", *Hydrology and Earth System Sciences*, vol. 1, No.3, pp. 523-534, 1997.

[7] Kriegler, F.J., Malila, W.A., Nalepka, R.F., and Richardson, W., "Preprocessing Transformations and Their Effects on Multispectral Recognition," *Proceedings of the Sixth International Symposium on Remote Sensing of Environment*, pp. 97-131, 1969.

[8] Green E.P., Mumby P.J., Edwards A.J., Clark C.D., and Ellis A. C. "Estimating Leaf Area Index of Mangroves from Satellite Data," *Aquatic Botany*, Vol. 58, Issue 1, pp. 11-19, 1997.

[9] Leguedois, S., Ellis, T. W., Hairsine, P. B., Tongway, D. J., "Sediment Trapping by a Tree Belt: Processes and Consequences for Sediment Delivery," *Hydrological Processes*, Vol. 22, Issue 17, pp. 3523–3534, 2008.

[10] Lin, Bor-Shiun "Estimation of Sediment Discharge and Trapping Efficiency in Shih-Men Watershed from LiDAR Technology", *The Young Southeast Asia Geotechnical Conference*, Taipei, Taiwan, May, 9~12, 2010.

[11] Hsiao, Cheng-Yang, Hsieh, Pao-Shan and Chi, Shu-Yuon, "Assessing Volume Earthwork by Using Unconventional Photogrammetry," *The Second World Landslide Forum*, 2011.